Carbon and oxygen isotopes of Maastrichtian–Danian shallow marine carbonates: Yacoraite Formation, northwestern Argentina

Rosa Marquillas, Ignacio Sabino, Alcides Nobrega Sial, Cecilia del Papa, Valderez Ferreira, Stephen Matthews

PII: S0895-9811(07)00038-7
DOI: 10.1016/j.jsames.2007.02.009
Reference: SAMES 692

To appear in: *Journal of South American Earth Sciences*

Please cite this article as: Marquillas, R., Sabino, I., Sial, A.N., Papa, C.d., Ferreira, V., Matthews, S., Carbon and oxygen isotopes of Maastrichtian–Danian shallow marine carbonates: Yacoraite Formation, northwestern Argentina, *Journal of South American Earth Sciences* (2007), doi: 10.1016/j.jsames.2007.02.009

Carbon and oxygen isotopes of Maastrichtian–Danian shallow marine carbonates: Yacoraite Formation, northwestern Argentina

Rosa Marquillas[1,2,*], Ignacio Sabino[1,2], Alcides Nobrega Sial[3], Cecilia del Papa[1], Valderez Ferreira[3], Stephen Matthews[4]

[1]CONICET, Buenos Aires 177, 4400 Salta, Argentina

[2]Universidad Nacional de Salta, Buenos Aires 177, 4400 Salta, Argentina

[3]NEG–LABISE, Department of Geology, UFPE, C.P. 7852 Recife, Brazil, 50670-000

[4]SERNAGEOMIN, CC 10465, Santiago, Chile

*Contact author

E-mail address: ramarq@unsa.edu.ar (R. Marquillas)

Abstract

The Maastrichtian–Danian limestones of the Yacoraite Formation (northwestern Argentina) show carbon and oxygen isotopic values consistent with shallow marine conditions. The members of the formation respond to different sedimentary environments and are characterised by distinctive stable isotopes and geochemistry. The basal Amblayo Member is composed of high-energy dolomitic limestones and limestones with positive isotopic values (+2‰ $\delta^{13}C$, +2‰ $\delta^{18}O$). The top of the member reveals an isotopic shift of $\delta^{13}C$ (-5‰) and $\delta^{18}O$ (-10‰), probably related to a descent in the sea level. The sandy Güemes Member has isotopically negative (-2‰ $\delta^{13}C$, -1‰ $\delta^{18}O$) limestones, principally controlled by water mixing decreased organic productivity, and compositional changes in the carbonates. The isotopically lighter limestones are calcitic, with a greater terrigenous contribution and different geochemical composition (high Si-Mn-Fe-Na, low Ca-Mg-Sr). These isotopic and lithological changes relate to the Cretaceous–Palaeogene transition. The Alemanía Member, composed of dolomitic limestones and pelites, represents a return to marine conditions and shows a gradual increase in isotopic values, reaching values similar to those of the Amblayo Member. The Juramento Member, composed of stromatolite limestones, shows isotopic variations that can be correlated with the two well-defined, shallowing upward sequences of the member.

Keywords: C and O isotopes, Northwestern Argentina, Yacoraite Formation, Shallow marine carbonates, K-T boundary

Resumen

Las calizas maastrichtiano-danianas de la Formación Yacoraite del noroeste argentino revelan valores de isótopos estables coherentes con el ambiente marino somero predominante del depósito. Los miembros de la Formación, que responden a variaciones ambientales, quedan caracterizados por valores isotópicos y geoquímicos. El Miembro Amblayo basal está compuesto por calizas dolomíticas y calizas de alta energía con valores isotópicos positivos (+2‰ $\delta^{13}C$, +2‰ $\delta^{18}O$). En el techo del miembro se observa un salto isotópico del $\delta^{13}C$ (-5‰) y del $\delta^{18}O$ (-10‰) probablemente vinculado con un descenso del nivel del mar. El Miembro Güemes, arenoso, posee calizas con valores isotópicos negativos (-2‰ $\delta^{13}C$, -1‰ $\delta^{18}O$) controlados principalmente por mezcla de aguas, descenso en la productividad orgánica y cambios composicionales del carbonato. Las calizas isotópicamente más livianas son calcíticas, poseen mayor contenido de elementos terrígenos y composición geoquímica diferente (alto Si-Mn-Fe-Na, bajo Ca-Mg-Sr). Estos cambios estarían relacionados con la transición Cretácico-Paleógeno. El Miembro Alemanía, compuesto por calizas dolomíticas y pelitas, representa un regreso a las condiciones marinas y muestra un paulatino aumento isotópico hasta asemejarse a los valores del Miembro Amblayo. El Miembro Juramento, compuesto por calizas estromatolíticas, muestra variaciones isotópicas que serían correlacionables con los dos ciclos de somerización bien definidos del miembro.

Palabras Clave: Isótopos de C y O, Noroeste Argentino, Formación Yacoraite, carbonatos marinos someros, Límite K-T

1. Introduction

The Yacoraite Formation (Maastrichtian–Danian) of the Salta Basin represents a carbonate deposit widely distributed in northwestern Argentina (Fig. 1). Despite having been the subject of diverse reviews (e.g., Castaños et al., 1975; Marquillas, 1985; Gómez Omil et al., 1989; Salfity and Marquillas, 1994; Marquillas et al., 2005), isotopic studies of this formation are still scarce (Matthews et al., 1996; Sial et al., 2001). The present study offers a new oxygen and carbon isotope analysis of whole-rock samples from the Metán subbasin and compares it with those of the Sey and Tres Cruces subbasins (Fig. 1). The Yacoraite Formation displays different carbonate and clastic lithofacies resulting from environmental changes during its accumulation (Marquillas, 1985, 1986). On the basis of these characteristics, four lithostratigraphic units (members) have been identified in the Metán subbasin (Fig. 2) (Marquillas and Salfity, 1989). The isotopic results herein are interpreted and discussed for each member.

1.1. Geological setting

Sedimentary deposits of the Salta Group (Neocomian–Palaeogene) are extensively distributed in the Andean to sub-Andean region of northwestern Argentina (Marquillas and Salfity, 1988; Marquillas et al., 1993; Salfity and Marquillas, 1994). The Yacoraite Formation (Maastrichtian–Danian) is a lithostratigraphic unit accumulated during the initial stage of thermal subsidence of the Salta rift (Marquillas et al., 2005). The Yacoraite Basin (Fig. 1) records the marine incursion at the end of the Cretaceous in most of South America (Zambrano, 1981, 1987; Riccardi, 1988; Salfity and Zambrano, 1990). The main lithology of the formation is carbonate—calcareous and dolomitic—but also contains shale and sandstone (Figs. 2, 3). The maximum thickness is 200 m.

The depositional environment of the Yacoraite Formation has long been discussed (Castaños et al., 1975; Marquillas, 1985, 1986; Gómez Omil et al., 1989; Salfity and Marquillas, 1994; Marquillas et al., 2005). The isotopic study in the present contribution confirms the marine character of the deposit, in opposition to other proposals that point to a continental origin (Hernández et al., 1999; Palma, 2000). Nevertheless, the paleontological evidence (e.g., euryhaline invertebrate association composed of ostracodes, bivalves, gastropods, and foraminifers and different types of charophytes) indicate shallow marine conditions and localized mixing of fresh and brackish water (see the paleontological record in Marquillas et al., 2005).

On the basis of their lithological features, several members can be identified within the Yacoraite Formation in the southern subbasins (Alemanía and Metán, Fig. 1). Members that are more extensively distributed are, from base to top, the Amblayo, Güemes, Alemanía, and Juramento (Fig. 2) (Reyes, 1972; Marquillas and Salfity, 1989). The Amblayo Member, composed of limestone and dolomitic limestone (Marquillas et al., 2000), constitutes the base of the Yacoraite Formation and is the thickest and most extensively distributed in the basin (Fig. 4a). The Güemes Member (Fig. 4b) comprises grey to whitish or brown to reddish sandstones and minor limestone levels. The Alemanía Member is a succession of grey dolomitic limestones and green shales (Fig. 4c). The Juramento Member is a thin, extensively distributed level of grey limestone at the top of the formation. The Yacoraite Formation in the Sey and Tres Cruces subbasins (Fig. 1) is calcareous and clastic (Marquillas et al., 1993), in which terrigenous components sometimes predominate, especially in sections at the margins of the basin, where it is not always possible to identify all the members (Fig. 3).

1.2. Age control

The age of the Yacoraite Formation is Maastrichtian–Danian (Marquillas, 1985), which implies that the Cretaceous–Tertiary transition occurred during its accumulation. The formation contains Senonian dinosaur tracks (Alonso and Marquillas, 1986) and

Maastrichtian and Danian palynomorphs (Moroni, 1982). The overlying Tunal Formation, according to its palynologic content, is Danian and includes *Mtchedlishvilia saltenia,* which defines a palynozone of Danian age (Quattrocchio et al., 2000). However, the precise location of the K-T boundary is still uncertain. Unfortunately, no biostratigraphic studies for Yacoraite Formation have been made to date. The sedimentary and geochemical studies carried out thus far have led to the conclusion that the K-T transition probably occurred during the accumulation of the middle Yacoraite Formation (Marquillas et al., 2002). In the Güemes Member (Fig. 2), an 8 m thick clastic section of anomalous Cr-Co-Ni content was identified, where the K-T boundary supposedly is located (Marquillas et al., 2003).

1.3. Previous isotope studies

Matthews et al. (1996) performed a petrographic, geochemical, and isotopic study of diverse samples of the Yacoraite Formation from the Sey and Tres Cruces subbasin (Fig. 1) and the calcsilicate xenoliths that occur in some lavas and pyroclastic flows of the Lascar Volcano of northern Chile. Matthews et al. (1996) find a positive correlation in the oxygen and carbon isotopes between the Yacoraite limestones and the calcite from the mentioned xenoliths.

Sial et al. (2001) sample two sections of limestones of the Yacoraite Formation at Maimará and Cabra Corral (Fig. 1). These two localities yield similar C-isotope stratigraphic profiles; $\delta^{13}C$ values of limestones of the Yacoraite Formation are essentially positive with values up to +2‰. In both sections, these authors find a strong shift in the $\delta^{13}C$ values (around -5‰). At the Cabra Corral section, this marked negative excursion is followed by a gradual increase of $\delta^{13}C$ values. These authors compare this isotopic behaviour with some places where the K-T boundary was determined. In addition, Sial et al. (2001) observe that the two sections studied display similar oxygen isotope behaviour, with gradual upward decreases of $\delta^{18}O$ toward the supposed K-T transition. They consider the oxygen isotope record to be near primary values, implying a substantial temperature increase and subsequent decrease around the K-T transition.

2. Sedimentary features of the Vacoraite Formation

The deposit of the Yacoraite Formation, as in most carbonate settings, was affected by early diagenetic processes (Bathurst, 1971), which tend to lead to mineral stabilisation and imprint their specific signs on the limestones. Different processes of variable intensity and selective occurrence, such as cementation, dissolution, recrystallisation, neomorphism, and dolomitization, have been noted in the Yacoraite limestones (Marquillas, 1985). However, original textures have been preserved to the extent of permitting reliable identification and interpretation of the facies and microfacies.

2.1. Sedimentary facies and depositional paleoenvironment

Several sedimentary facies characterise the Yacoraite Formation (Marquillas et al., 2003; Marquillas and del Papa, 2003). Their summary descriptions follow.

2.1.1. Grainstone facies. Grey oolitic and intraclastic limestones constitute this facies. It shows thin to thick stratification, tabular strata with erosive bases and intraclasts at the base, and undulate tops, parallel and cross-lamination, and current and wave ripples. The rocks are sparry limestones with spherical normal (Fig. 4d) or composite oolites (one to three nuclei) (Fig. 4e). The intraclasts are micritic, flat, and long (2–4 mm), and the majority are oolitized with at least one carbonate envelope, which is a typical facies of the Amblayo Member (Fig. 4a) and is also observed in part of the Alemanía Member (Fig. 4c). This facies points to high- to moderate-energy depositional conditions, with permanent wave agitation of the water.

2.1.2. Calcareous mudstone–wackestone facies. Grey calcareous mudstones, dolomicrites, and grey to greenish bioclastic wackestones constitute this facies. It consists of internally laminated—sometimes massive as a result of bioturbation—tabular or lenticular strata. The limestones are very homogeneous micrites and microspars, with some spar-filled voids, abundant ostracodes, miliolid foraminifers (Fig. 4f), gastropods, and phosphatized remains of fish. This facies is common in the Alemanía Member (Fig. 4c) and in the upper part of the Amblayo Member (Fig. 4a) and less frequently constitutes thin levels of the Güemes Member (Fig. 2). It is also present in several profiles of the Sey subbasin (Fig. 1). The facies points to a low-energy setting, with decantation of fine material beneath the base level of the waves. The alternation of beds with signs of organic activity and laminated levels indicates fluctuating oxic conditions.

2.1.3. Green and black shale facies. Green and black shales, light green to grey mudstones, and fine-grained siltstones constitute this facies. It shows tabular, internally laminated or massive strata with evidence of bioturbation. Organic matter and hydrocarbons are common. Gypsum laminae are occasionally present. This facies is frequently associated with stromatolites (Fig. 4g) and constitutes part of the shallowing upward sequences (Fig. 4c) of the Alemanía Member. The green and black shale facies indicates low-energy conditions in which fine material settled down beneath the base level of the waves.

2.1.4. Heterolithic limestone facies. Grainstones, fine-grained packstones, wackestones, and micrite laminae characterise this facies (Fig. 4h). The strata show wavy and flaser stratification. The wackestones and packstones include oolites, intraclasts, broken bivalves, ostracodes, foraminifers, and phosphatized bones. The facies can contain fine, disseminated detrital material, scattered organic matter, and some pyrite crystals. It is typical of the Alemanía Member (Fig. 4c), also defined in the Amblayo Member (Fig. 4a). This facies suggests energy fluctuating from moderate to low conditions with alternating traction and

decantation processes. The tractive or suspension domains produce flaser or lenticular structures. The bioclastic remains indicate moderate- to high-energy conditions and may represent episodic storms.

2.1.5. Stromatolite facies. This facies is made up of grey to yellowish limestones in dome structures that form continuous beds. Dome heights can vary from 3 to 120 cm, with 25–30 cm domes being the most abundant (Fig. 4g). The dome specimens are concentrically laminated and show close lateral linkage, sometimes with brecciated surfaces and mudcracks. The laminae consist of dolomite, sparry and fibrous microsparry calcite (Fig. 4i), micrite, and gypsum. This facies is characteristic of the Juramento and Alemanía members (Fig. 2), where it is part of the cyclic deposits of the shallowing-upward sequences (Fig 4c). Less abundantly, stromatolites constitute part of the Amblayo Member (Fig. 4a) and also the column of the Yacoraite Formation in the Sey and Tres Cruces subbasins (Fig. 1).

2.1.6. Packstone with HCS facies. Tabular bioclastic and intraclastic packstone strata with hummocky cross stratification (HCS) (Fig. 4j) represent this facies. It contains bivalves, articulate and disarticulate ostracodes, fragments of algae, and micritic intraclasts aligned in the cross-lamination. It also exhibits laminae with abundant terrigenous material (quartz and mica) that form continuous levels intercalated with carbonate material (Fig. 4k). This facies characterises the top of the Amblayo Member (Fig. 4a) and has been interpreted as tempestites accumulated during successive storm episodes.

2.1.7. Gray and white calcareous sandy facies. Formed of fine- to medium-grained calcareous sandstone containing mostly quartz and minor K-feldspar, this facies frequently contains intraclasts and lithic clasts in the Sey subbasin (Fig. 4l). Sometimes it is coarse-grained calcareous sandstones, and it is thickly stratified. This facies constitutes part of the lower section of the Yacoraite Formation in the Sey and Tres Cruces subbasins (Fig. 1) and is common at the base of the formation in the Metán subbasin. Frequently, the sandy beds are related to oolitic grainstone that represents high-energy episodes.

2.1.8. Silty red sandstone facies. This facies is composed of coarse strata and structureless or stratified fine-grained red sandstones, with pelitic and carbonate clasts. It is a fine-grained wacke containing quartz, mica, phosphatic fishbone fragments, and abundant iron oxide (Fig. 4m) and oxidised pyrite crystals. The tops of the beds display marks of bioturbation and current ripples. This facies has been interpreted as resulting from combined episodic low- and high-density flows. When structureless, it is interpreted as a product of density flow; flow decay and subsequent fluid behaviour then generated ripple structures. The silty red sandstone facies is typical of the Güemes Member (Fig. 4b) in the Metán subbasin

(Fig. 1). This facies probably accumulated in a transitional environment, in which some influence of continental water is not discarded.

The depositional environment of the Yacoraite Formation corresponds, in general, to a restricted shallow sea controlled by different processes (Marquillas et al., 2005): The beginning of the Maastrichtian deposition was dominated by intertidal action (Amblayo Member), followed by storm-dominated action (top of the Amblayo Member), with a likely period of continental to transitional sedimentation (Güemes Member). Finally, the depositional system was controlled by fairweather waves (Alemanía and Juramento members).

3. Methods and analytical techniques

Three hundred fifty samples were collected from the Yacoraite Formation in several sections of the Metán subbasin (Fig. 1). From this sampling, 39 subsamples were chosen for C and O isotope analyses. These samples were screened after examination in thin sections under a polarising microscope (National University of Salta, Argentina) and analysed by X-ray fluorescence (Federal University of Pernambuco, Brazil). Samples with strong diagenesis signals were eliminated.

The analyses were performed on whole-rock samples. They are micritic, sparry, and stromatolite limestones. Semi-quantitative dolomite/calcite ratios were obtained by X-ray diffraction analysis in the LANAIS Laboratory at the National University of Salta, with a maximum error of 2%. The limestones of the Yacoraite Formation are often dolomitic in a variable percentage (up to 86%) (Marquillas, 1985; Marquillas et al., 2000); therefore, about half of the analysed samples correspond to dolomitic limestones (>10% dolomite, Table 1).

The C and O isotope analyses, employing the conventional digestion method (McCrea, 1950), were performed at the Stable Isotope Laboratory (LABISE), Federal University of Pernambuco, Brazil. Powdered samples were reacted with 100% H_3PO_4 at 25°C for one day to release the CO_2. An extended reaction period was preferred for the dolomites (three days) rather than increasing the reaction temperature. The $\delta^{13}C$ and $\delta^{18}O$ values were measured on cryogenically cleaned CO_2 (Craig, 1957) in a triple collector SIRA II mass spectrometer. The C and O isotopic data are presented as deviations with reference to PDB. Borborema skarn calcite (BSC), calibrated against international standards, was used as the reference gas, and reproducibility of the measurements was generally better than ± 0.1‰. The values obtained for the standard NBS-20 in a separate run against BSC yield $\delta^{13}C_{PDB}$ = -1.05‰, and $\delta^{18}O_{PDB}$ = -4.22‰, which are in close agreement with the values reported by the U.S. National Bureau of Standards (-1.06‰ and -4.14‰, respectively). The external precision based on multiple standard measurements of NBS-19 is better than 0.1‰ for carbon and oxygen. For XRF

analyses, fused beads were prepared using Li fluoride and Li tetraborate, and uncertainties based on the measurement of multiple standard materials by this method are greater than 5% for Sr and Fe and 10% for Mn.

In addition, this study includes 18 whole-rock analyses of low-magnesium limestones from the Sey and Tres Cruces subbasins. These samples were analysed in the Stable Isotope Laboratory at Royal Holloway College (London, UK) (Matthews et al., 1996).

4. Stable isotopes

The limestones of the Yacoraite Formation basin exhibit $\delta^{13}C$ values from -2.5‰ to 2.5‰ in the Metán subbasin (Table 2), a characteristic range for Cretaceous marine limestones and dolomitic limestones (Hudson, 1977; Moss and Tucker, 1995; Ayyildiz et al., 2004). However, some samples from the Sey and Tres Cruces subbasins (Fig. 1) that display values between -5‰ and 4‰ also were recorded (Tables 3, 4). The oxygen isotope behaviour is more variable than that of the carbon isotope, with values ranging from -10‰ to 4‰.

In the Metán subbasin (Fig. 1), the four members of the Yacoraite Formation (Fig. 2) show distinct isotope attributes (Fig. 5). The $\delta^{18}O$ values are positive in the Amblayo and Alemanía members. The Güemes and Juramento members show negative values (<-1‰). The most positive C and O isotope values are observed in the Amblayo Member, and they decrease toward the top. However, both isotopes decrease suddenly in the upper 7 m of the Amblayo Member, reaching the most negative values of the Yacoraite Formation; only one sample (K-L) indicates a positive value (Fig. 2). The carbon and oxygen isotopes at the top of the Amblayo Member show a positive correlation (Fig. 5).

For the Güemes Member, both $\delta^{18}O$ and $\delta^{13}C$ are negative with minor fluctuations; the $\delta^{13}C$ shows, on average, more negative values (Fig. 5). At its base, the limestones interbedded with red sandstones are isotopically higher than those at the top, which are interbedded with green sandstones. Sample C316 presents isotopic values intermediate between the Güemes and Alemanía members, revealing the transition between them (Fig. 5). The isotopic changes noted at the top of the Amblayo Member and in the Güemes Member coincide with geochemical changes—notably, the absence of dolomite; the decrease of Mg, Ca, and Mg/Ca; and increased Mn contents, Mn/Sr ratios, P, and, particularly Si, Al, and Fe (Fig. 6).

In the Alemanía Member, $\delta^{13}C$ oscillates between -2.3‰ and 1.5‰, the greatest fluctuation of C isotopes. $\delta^{18}O$ are positive, usually between 0.5‰ and 2‰. Two samples (C701 and E16) exhibit $\delta^{18}O$ values up to 3.8‰, with a high Fe-dolomite content (Dol/Calc > 70%, Table 1) and gypsum laminae (E16). One sample from the top of the Alemanía Member (E30) has intermediate values between those typical of the Juramento and Alemanía members (Fig. 5). The Juramento Member exhibits limited variation of $\delta^{13}C$ (-0.8 to 0.4‰), though it

shows the largest variation of $\delta^{18}O$ (-2 to -6‰). Two samples of the lacustrine Tunal Formation (Fig. 2), which conformably overlies the Juramento Member of the Yacoraite Formation, also were analysed. The $\delta^{13}C$ values observed in the Tunal Formation are relatively low (Table 2, Fig. 5). The Tunal Formation is composed of green shale facies similar to the Alemanía and Juramento members; the main difference appears in the frequent evaporites and scarce carbonates (dolomicrites).

In the Sey and Tres Cruces subbasins (Fig. 1), the Yacoraite Formation shows isotope ratios between 0 and -5.7‰ for $\delta^{13}C$ and between +3 and -6.7‰ for $\delta^{18}O$. Sampling density is poor in these areas due to the difficult access and poor quality of the outcrops. In this area, only the Huaytiquina section (Fig. 3) has been sufficiently analysed to observe vertical isotopic variations.

Environmental variations were recorded in the different lithologic members of the Yacoraite Formation (Fig. 2). Each member represents a discrete population in the $\delta^{18}O$ versus $\delta^{13}C$ plot, where an isotopic transition within the domain of each field is observed (Fig. 5). The distribution is coherent with the environmental interpretation from the sedimentary facies (Fig. 5). In general, the values are typical for marine limestones and dolomites, except in some samples of the Sey and Tres Cruces subbasins (Fig. 1, Tables 3, 4), in which the formation consists of sandstones, calcareous sandstones, pelites, and scarce limestones due to their marginal position. In the upper part of the Huaytiquina section (Fig. 3), very negative $\delta^{13}C$ values are recorded. In general, the highest $\delta^{13}C$ values correspond to the basal portion of each section, as observed in the Huaytiquina profile (Fig. 3) and the Metán subbasin (Fig. 2).

In the Metán subbasin, the Yacoraite limestones are mainly dolomitic. The dolomitic samples of the Amblayo and Alemanía members display positive $\delta^{18}O$ values (Table 2). The isotopic values of the Amblayo Member dolomitic limestones (Fig. 5) coincide with the common range of marine dolomites, especially the values for mixing zone dolomites (Fig. 7). The dolomicrites of the overlying Tunal Formation show isotopic values coherent with the lacustrine environment (Novara, 2003). The limestones (without dolomite) at the top of the Amblayo Member decrease in isotopic values, reaching a field that corresponds to freshwater limestones (Fig. 5). This decrease coincides with the transition between the Amblayo and Güemes members and implies a major change in environmental conditions. The isotopic values of the Güemes Member limestones occupy an intermediate position between the marine and freshwater fields (Fig. 5), probably as a result of the interaction between seawater and freshwater. The Juramento Member (Fig. 2) is composed of two shallowing-upward

sequences (not represented in Fig. 2 for scale); the decrease in $\delta^{13}C$ and $\delta^{18}O$ values could be related to the maximum shallowing of the environment at the end of each sequence.

5. Geochemistry

The Sr content in the Yacoraite limestones is usually high, often up to 1200 ppm, ranging from 328 to 24000 ppm (Table 1). Macrocrystals of diagenetic strontian–barite were identified in samples with Sr greater than 5000 ppm. Ancient dolomites exhibit Sr contents between 150 and 300 ppm; scarce examples with more than 750 ppm are interpreted as products of a water-buffered system with a high Sr/Ca ratio derived from the dissolution of aragonite (Veizer, 1990; Budd, 1997). Most Yacoraite limestones are interpreted as originally aragonitic and calcitic; nevertheless, some primary dolomite precipitation is not discarded (Marquillas, 1985; Marquillas and Matthews, 1998). The contents of Mn (150–2000 ppm) and Fe (0.3–5%) are also high (Table 1), which implies reducing conditions of the pore water (Budd, 1997). The presence of biotite, tourmaline, vermiculite, and illite in the detrital fraction suggests that these minerals were a significant external source for the Fe content.

The Mn/Sr ratio is low, usually close to 1, and in only one case (L06 of the Güemes Member; Mn/Sr = 4.4) does it reach higher values. A similar pattern was noted by Sial et al. (2001). Kaufman et al. (1993) and Kaufman and Knoll (1995) demonstrate that Mn/Sr is useful for screening samples because, under the influence of meteoric fluids, Sr is expelled from marine carbonates while Mn is incorporated. They suggest that carbonates (both limestones and dolomites) with Mn/Sr < 10 commonly retain near-primary $\delta^{13}C$ abundance.

The application of this parameter permits a comparatively precise determination of the degree of alteration of C-isotopic values, because the volumes of meteoric fluid that could easily alter Mn/Sr may have no effect on major element chemistry. The relative increase in the Mn/Sr ratio at the top of the Amblayo Member and the lower Güemes Member is probably related, among other factors, to the influence of the early meteoric diagenesis.

In the Yacoraite Formation, sodium (0–4%) and potassium (0–2.65%) contents show a correlation with silica content (Fig. 8), which is due to the detrital fraction origin of these elements, especially micas and feldspars. Samples with high sodium/silica or potassium/silica ratios (e.g., E16, C701, K-L) reflect the presence of evaporate laminae, whereas those with an abnormally low ratio (e.g., C402, C812) relate to the occurrence of silicified bone fragments or oolite nuclei.

6. Environmental implications

6.1. Amblayo and Güemes members

Moderate- to high-energy dolomitic limestones and limestones (grainstone, packstone with HCS, and minor heterolithic limestone facies) accumulated during the deposition of the

Amblayo Member. The average $\delta^{13}C$ for this member is +1‰, similar to Maastrichtian marine carbonates from England (Jenkyns et al., 1994). Positive $\delta^{18}O$ values are common in ancient dolomitic limestones (Veizer and Hoefs, 1976; Budd, 1997). In the $\delta^{18}O$ versus $\delta^{13}C$ diagram (Fig. 5), the samples of the Amblayo Member are located in fields typical of marine dolomitic limestones (Budd, 1997; Warren, 2000). The facies association and isotopic values of the Amblayo Member suggest definite marine conditions, coincident with the beginning of the Maastrichtian transgression, and a gradual restriction toward the top of the member (Figs. 2, 5).

The isotopic shift observed in carbonates at the top of the Amblayo Member probably relates to a sudden change in the initial conditions of sedimentation and the effects of early meteoric diagenesis. The upper 7 m of the Amblayo Member reveal an increase in terrigenous content (Fig. 6). These new conditions were maintained during the accumulation of the Güemes Member, characterised by silty red sandstone facies and mudstone-wackestone facies. The 18 m thick Güemes Member shows high participation of detrital components. The top of the Amblayo Member and the Güemes Member represent the stage of greatest sea restriction. In addition, the mudcracks, breccias ,and intraclasts indicate a low marine level. A coincident increase in phosphate contents is observed (Fig. 6). Carbon and oxygen isotope values show a rapid decrease at the top of the Amblayo Member. The lowest $\delta^{18}O$ value (-10‰) occurs below the contact between the Amblayo and Güemes members (Fig. 2). The sedimentary facies near the contact (Fig.1) records a progressive shallowing process that probably reached sub-aerial exposure, though no palaeosols have been observed. The occurrence of a non-isotopically homogeneous profile and the lack of pedogenetic evidence suggest a brief sub-aerial exposure, as has been reported for both ancient and modern carbonate deposits (Allan and Matthews, 1982; Joachimski, 1994), in which exposition levels show an abrupt decrease in the C and O heavy stable isotopes.

In the Güemes Member, oxygen isotope values are consistently low (-2.5‰ average), perhaps due to the efficient mixing of freshwater, usually isotopically light (-2 to -15‰, Dickson, 1992). This mixing also could have influenced the lower values of the carbon isotope, though it may be associated with relatively lower organic productivity (Tucker, 1992). The Güemes Member begins with fine-grained red sandstones accumulated in rapid sedimentation events (Marquillas et al., 2003) with scarce limestone intercalations. The limestones at the base of the member exhibit higher $\delta^{13}C$ values than the limestones at the top. Positive excursions of $\delta^{13}C$ and $\delta^{18}O$ have been reported in red calcareous facies associated with epeiric seas by Immenhauser et al. (2003).

The isotopic variation observed at the top of the Amblayo Member and in the Güemes Member coincides with geochemical changes in the limestones (Fig. 6). The absence of dolomite is notable and coincides with decreased Mg/Ca ratios and Mg contents. Marine dolomites usually have positive oxygen isotopes, unlike marine limestones, whose values are close to zero or slightly negative. The increased Mn and Mn/Sr ratios also relate to modification in carbonate composition, whereas the considerable increase in Si, Al, and Fe and decreased Ca indicate an increase in clastic components and decrease in total carbonate. The rise in P contents may be associated with the remains of fish bones and the clastic apatite observed.

The basal section of the Güemes Member shows anomalies of siderophile elements compatible with the K-T boundary (Marquillas et al., 2002, 2003). The Yacoraite limestones show strong negative excursion of $\delta^{13}C$ values, close to the stratigraphic inferred position of the K-T boundary, which correlates with a decrease in carbonate content and a peak of the transition element concentration. This isotopic behaviour has been documented in three subbasins of the Yacoraite basin (Fig. 1): Sey, Metán (this study), and Tres Cruces (Sial et al., 2001).

The regressive event recorded at the end of the accumulation of the Amblayo Member can be associated with the major sea-level fall at 100–50 Ka before the K-T transition in some shallower marine regions (Keller and Stinnesbeck, 1996; Hallam and Wignall, 1999).

In the Cabra Corral section, Sial et al. (2001) erroneously identify the base of the Güemes Member as the base of the Tunal Formation, where they assume the K-T transition to be (see also the discussion in Marquillas et al., 2003). Sial et al. (2001) interpret the gradual decrease of $\delta^{18}O$ toward the supposed K-T transition in this section, resulting from a substantial temperature increase and subsequent decrease around the K-T transition. However, mixing of marine and continental waters occurred in the broad Yacoraite basin (Marquillas, 1986), which implies changes in the oxygen-isotope composition of the water and limits the use of oxygen isotopes in determining the palaeothermometry with which carbonates equilibrated isotopically.

In the South Atlantic where K-T was determined, the shift in carbon and oxygen isotopes is similar to that noted here (Hsü, 1986; Magaritz, 1989). This behaviour is concordant with that reported for the Pernambuco-Paraíba basin, in northeastern Brazil (Ferreira et al., 1994). The $\delta^{13}C$ pattern shows an important drop from +2‰$_{PDB}$ to -5.5‰$_{PDB}$ at the K-T transition from the Gramame to the Maria Farinha Formation limestones, accompanied by an increase in $\delta^{18}O$ (from -4 to -1‰$_{PDB}$), corresponding to an important temperature drop at the transition (Ferreira et al., 1994). A $\delta^{13}C$ negative excursion also is

recorded in other K-T boundary sections at low latitudes (Keller and Lindinger, 1989; Zachos et al., 1989; Li and Keller, 1998; Abramovich et al., 2002).

6.2. Alemanía and Juramento members

The Alemanía Member represents a return to normal marine conditions, as documented by sedimentary facies. This member differs from the basal Amblayo Member in the large amount of pelites, which constitute about half its thickness. The Alemanía Member is composed of green and black shale, mudstone-wackestone, heterolithic limestone, grainstone, and stromatolite facies arranged in shallowing-upward sequences (Marquillas and del Papa, 2003; Marquillas et al., 2005). The lower Alemanía Member (Fig. 2) is composed of dark-green and black shales often rich in organic matter and a low proportion of carbonate rocks, which implies low carbonate production. It is coincident with the lowest $\delta^{13}C$ values (Fig. 2). The proportion of carbonate increases toward the top, where the limestones and stable isotopes (e.g., E21, C812) are similar to those of the Amblayo Member (Figs. 2, 5). The gradual change of $\delta^{13}C$ of the Alemanía Member records the return to marine conditions similar to those of the Amblayo Member (Fig. 5).

The Juramento Member limestones have low $\delta^{18}O$ values, probably representing the most important influence of freshwater in the basin's depositional history. This member is in contact with the lacustrine Tunal Formation, which can be distinguished by its low $\delta^{13}C$ values (Fig. 2). The Juramento Member differs from the Güemes Member in the lower participation of detrital components and the absence of silty red sandstone facies. Carbon isotope behaviour in the Juramento Member is similar to that observed in the Alemanía Member, reflecting similar facies in these two units.

The Juramento Member, dominated by stromatolite facies, comprises two shallowing-upward sequences, each of which shows an isotopic variation coherent with the sedimentary processes at this scale, though data are still scarce. The carbon and oxygen isotopes decrease toward the top of the sequence, where evidence of sub-aerial exposure is common (mudcracks, breccias, etc.). This upward isotopic decrease is also described for the shallowing-upward sequences in the Early Cretaceous (Joachimski, 1994).

6.3. Yacoraite Formation in the Sey and Tres Cruces subbasins

In samples from the Sey subbasin (western Yacoraite basin) and Tres Cruces subbasin (northwestern Yacoraite basin) (Fig. 1), isotope behaviour typical of marine to freshwater limestones is observed (Fig. 7). Here, the formation shows a higher clastic input, especially at the marginal areas, where it is dominated by sandy calcareous facies and minor mudstone-wackestone, stromatolite, and heterolithic limestone facies. The Yacoraite Formation of the Sey subbasin in Huaytiquina comprises two lithologically distinct sections (Fig. 3): The lower

portion is dominated by limestones with stable isotopes showing marine values (Z = 128–134), whereas the upper is pelitic with scarce limestones. This lithological change is accompanied by a marked decrease in $\delta^{13}C$. The middle part of the column contains a layer of volcanic ash. To the west, in northern Chile (Fig. 1), a short-lived, intense compressive event has been identified between 65 and 62 (61?) Ma (Cornejo et al., 2003), which inverted the Campanian–Maastrichtian continental basins underlying the present-day north of Chile (Central Depression). During this event, both the basin fill strata and large blocks of underlying Jurassic "basement" were uplifted and eroded. Uplift and erosion may have controlled, among other things, the sedimentary input to the Yacoraite Formation in this part of the basin.

7. Conclusions

The present isotopic study ratifies the restricted marine environment of the Yacoraite Formation (Maastrichtian–Danian). The general isotopic behaviour of the deposit is as expected for a shallow marine setting.

Each lithologic member of the formation has a distinctive isotopic signature that varies in its carbonate composition (calcite-dolomite) and detrital content. The isotopic changes are transitional or subtly precede the facies changes that bind the different members.

The basal Amblayo Member records the main marine incursion, characterised by moderate- to high-energy dolomitic limestones and limestones enriched in heavy isotopes. A sharp increase in light isotopes occurs at the top. The isotopes and sedimentary facies in this stratigraphic position suggest a sudden lowering in sea level. The overlying clastic–calcareous Güemes Member is characterised by negative isotope values, interpreted as a consequence of the increase in terrestrial water input to the basin.

The sudden changes in carbon and oxygen isotopes, geochemistry, and the clastic facies may be related to the K-T boundary, which is interpreted as preserved between the upper Amblayo and basal Güemes members.

The positive isotopic values of the Alemanía Member attest to the return to normal marine conditions. In the uppermost Juramento Member, the isotopic variations coincide with the transition to continental facies in the upper Tunal Formation (Danian).

Notable variations in the lithologic and isotopic characteristics of the Yacoraite Formation are observed at the western limit of the basin. It is likely that the deposition in this part of the basin was influenced by a compressive deformation event that occurred in northern Chile between 65 and 62 Ma.

Acknowledgements

We appreciate the helpful comments of G. D. Price and H. Panarello. R. Marquillas, I. Sabino, and C. del Papa express their gratitude to FONCyT-ANPCyT (PICT 12419) and the CIUNSa–Universidad Nacional de Salta (Project 1220), Argentina, for their financial support. I. Sabino thanks CNPq-CONICET for a postdoctoral grant. We acknowledge Nilda Menegatti for X-ray determinations. A. N. Sial and V. P. Ferreira are grateful to Vilma S. Bezerra and Gilsa M. de Santana for their assistance with C and O isotope analyses at the Stable Isotope Laboratory (LABISE), Federal University of Pernambuco. This is NEG-LABISE contribution N. 231 and a INCE-UNSa contribution.

References

Abramovich, S., Keller, G., Adatte, T., Stinnesbeck, W., Hottiger, L., Stueben, D., Berner, Z., Ramanivosoa, B., Randriamanantenasoa, A., 2002. Age and paleoenvironment of the Maastrichtian to Paleocene of the Mahajanga Basin, Madagascar: a multidisciplinary approach. Marine Micropaleontology 47 17-70.

Allan, J.R., Matthews, R.K., 1982. Isotope signatures associated with early meteoric diagenesis. Sedimentology 29 797-817.

Alonso, R.N., Marquillas, R.A., 1986. Nueva localidad con huellas de dinosaurios y primer hallazgo de huellas de aves en la Formación Yacoraite (Maastrichtiano) del Norte Argentino. 4th Congreso Argentino de Paleontología y Bioestratigrafía, Actas 2 33-41. Mendoza.

Ayyildiz, T., Tekin, E., Satir, M., 2004. Water circulation near the mixed – water and microbiologic activity of the Mesozoic Dolomite Sequence, an example from the Central Taurus, Turkey. Carbonates and Evaporites 19 107-117.

Bathurst, R.G.C., 1971. Carbonate sediments and their diagenesis. Elsevier, New York.

Budd, D.A., 1997. Cenozoic dolomites of carbonate islands: their attributes and origin. Earth-Science Reviews 42 1-47.

Choquette, P.W., Steinen, R.P., 1980. Mississipian non-supratidal dolomite, Ste. Genevieve limestone, Illinois Basin: evidence for mixed-water dolomitization. In: Zenger, D.H., Dunham, J.B., Ethington, R.L. (Eds.), Concepts and models of dolomitization. SEMP Special Publication 28, pp. 163-196.

Cornejo, P., Matthews, S., Pérez de Arce, C., 2003. The "K-T" compressive deformation event in northern Chile (24-27·S). 10th Congreso Geológico Chileno, Resúmenes expandidos, Concepción.

Castaños, A., Pinedo, R., Salfity, J., 1975. Nuevas consideraciones sobre la Formación Yacoraite del Cretácico Superior del norte argentino. Revista Técnica Y.P.F. Bolivianos, Publicación Especial 4 (3) 31-59.

Craig, H., 1957. Isotopic standards of carbon and oxygen and correction factors for mass-spectrometric analysis of carbon dioxide. Geochimica et Cosmochimica Acta 12 133-149.

Dickson, J.A.D., 1992. Carbonate mineralogy and chemistry. In: Tucker, M.E., Wright, V.P. (Eds.), Carbonate Sedimentology. Blackwell Scientific Publications, London, pp. 284-313.

Ferreira, V.P., Sial, A.N., Chaves N.S., Brasilino R.G., 1994. Stable isotopes and the K-T boundary in the Pernambuco-Paraíba coastal Sedimentary basin, Northeastern Brazil.14th International Sedimentological Congress, S3 4-5. Recife.

Gómez Omil, R.J., Boll, A., Hernández, R.M., 1989. Cuenca cretácico-terciaria del Noroeste argentino (Grupo Salta). In: Chebli, G.A., Spalletti, L.A. (Eds), Cuencas Sedimentarias Argentinas. Universidad Nacional de Tucumán, Serie de Correlación Geológica 6, pp. 43-64.

Hallam, A., Wignall, P.B., 1999. Mass extinctions and sea level changes. Earth-Science Reviews 48 217-250.

Hernández, R.M., Disalvo, A., Boll, A., Gómez Omil, R., Galli, C., 1999. Estratigrafía secuencial del Grupo Salta, con énfasis en las subcuencas de Metán-Alemanía, Noroeste Argentino. 14th Congreso Geológico Argentino, Relatorio 263-283.

Hsü, K.J., 1986. Cretaceous/Tertiary boundary event. In: Hsü, K.J. (Ed.), Mesozoic and Cenozoic Oceans. Geodynamics Series 15, pp. 75-84.

Hudson, J.D., 1977. Stable isotopes and limestone lithification. Journal of the Geological Society of London 133 637-660.

Immenhauser, A., della Porta, G., Kenter, J.A.N., Bahamonde, J.R., 2003. An alternative model, for positive shifts in shallow-marine carbonate $\delta^{13}C$ and $\delta^{18}O$. Sedimentology 5 953-959.

Jenkyns, H.C., Gale, A.S., Corfield, R.M., 1994. Carbon- and oxygen-isotope stratigraphy of the English Chalk and Italian Scaglia and its palaeoclimatic significance. Geological Magazine 131 1-34.

Joachimski, M.M., 1994. Subaereal exposure and deposition of shallowing upward sequences: evidence from stable isotopes of Purbeckian peritidal carbonates (basal Cretaceous), Swiss and French Jura Mountains. Sedimentology 41 805-824.

Kaufman, A.J., Knoll, A.H., 1995. Neoproterozoic variations in the C-isotopic composition of seawater: stratigraphic and biogeochemical implications. Precambrian Research 73 27-49.

Kaufman A.J., Jacobsen, S.B., Knoll, A.H., 1993. The Vendian record of Sr- and C-isotopic variations in seawater: implications for tectonics and paleoclimate. Earth and Planetary Sciences Letters 120 409-430.

Keith, M.L., Weber, J.N., 1964. Carbon and oxygen isotopic composition of selected limestones and fossils. Geochimica et Cosmochimica Acta 28 1787-1816.

Keller, G., Lindinger, M., 1989. Stable isotope, TOC and $CaCO_3$ record across the Cretaceous/Tertiary boundary at the El Kef, Tunisia, Palaeogeography, Palaeoclimatology, Palaeoecology 73 243-265.

Keller, G., Stinnesbeck, W., 1996. Sea-level changes, clastic deposits, ans megatsunamis across the Cretaceous-Tertiary boundary. In: MacLeod, N., Keller, G. (Eds.), Cretaceous-Tertiary Mass Extinctions: Biotic and Environmental Change. Norton, London, pp. 415-449.

Li, L., Keller, G., 1998. Maastrichtian climate, productivity and faunal turnovers in planktonic foraminifera in South Atlantic DSDP sites 525A and 21. Marine Micropaleontology 33 55-86.

Magaritz, M., 1989. ^{13}C minima follow extinction event: a clue to faunal radiation. Geology 17 337-340.

Marquillas, R.A., 1985. Estratigrafía, sedimentología y paleoambientes de la Formación Yacoraite (Cretácico Superior) en el tramo austral de la cuenca, norte argentino. Doctoral Thesis, Universidad Nacional de Salta (Argentina).

Marquillas, R.A., 1986. Ambiente de depósito de la Formación Yacoraite (Grupo Salta, Cretácico-Eocénico), Norte argentino. 1st Simp Proyecto 242 PICG-UNESCO 157-173.

Marquillas, R.A., del Papa, C.E., 2003. Carbonate microfacies of the Yacoraite Formation (Maastrichtian-Danian) in the Metán subbasin, NW Argentina. 3rd Latin American Congress of Sedimentology, Abstracts Book 162-163. Belem

Marquillas, R.A., Matthews, S.J., 1998. Geoquímica de los travertinos de Huaytiquina, Puna argentina. 7th Reunión Argentina de Sedimentología, Resúmenes 86-87. Salta

Marquillas, R.A., Salfity J.A., 1988. Tectonic framework and correlations of the Cretaceous-Eocene Salt Group, Argentine. In: Bahlburg, H., Breitkreuz, Ch., Giese, P. (Eds.), The Southern Central Andes. Lecture Notes in Earth Sciences 17, Springer, Berlin-Heidelberg, pp. 119-136.

Marquillas, R.A., Salfity, J.A., 1989. Distribución regional de los miembros de la Formación Yacoraite (Cretácico Superior) en el noroeste argentino. Contribuciones de los Simposios sobre Cretácico de América Latina, Parte A, Eventos y Registro Sedimentario 253-272. Buenos Aires

Marquillas, R.A., Salfity, J.A., Monaldi, C.R., 1993. Regional development of the Salta Group facies in the Argentine Puna. International Symposium on Andean Geodynamics II. Oxford, Editions de L'Orstom, Collection Colloques et Séminaires 21-23.

Marquillas, R., Azarevich, M., Novara, M., Menegatti, N., Sabino, I., 2000. Relaciones calcita-dolomita de la Formación Yacoraite (Maastrichtiano) en El Chorro, provincia de Salta, Argentina. 2nd Latinoamerican Congress of Sedimentology, Abstracts 111-112.

Marquillas, R., del Papa, C., Sabino, I., Heredia, J., 2002. Stratigraphic record and geochemistry of the Yacoraite Formation, an approach to the K/T boundary in Northwest Argentina. 9th International Conference on Moldavites, Tektites and Impact Process, Field Trip Guidebook and Abstracts Book, Františkovy Lázne 41-42.

Marquillas, R.A., del Papa, C.E., Sabino, I.F., Heredia, J., 2003. Prospección del límite K/T en la cuenca del Noroeste, Argentina. Revista de la Asociación Geológica Argentina 58 (2) 271-274.

Marquillas, R.A., del Papa, C.E., Sabino, I.F., 2005. Sedimentary aspects and paleoenvironmental evolution of a rift basin: Salta Group (Cretaceous-Paleogene), northwestern Argentina. International Journal of Earth Sciences 54 94-113.

Matthews, S.J., Marquillas, R.A., Kemp, J.A, Grange, F.K., Gardeweg, M.C., 1996. Active skarn formation beneath Lascar Volcano, northern Chile: a petrographic and geochemical study of xenoliths in eruption products. Journal of Metamorphic Geology 14 509-530.

McCrea, J.M., 1950. On the isotopic chemistry of carbonates and a paleotemperature scale. Journal of Physical Chemistry 18 849-857.

Moroni, A.M., 1982. Correlación palinológica en las Formaciones Olmedo y Yacoraite. Cuenca del Noroeste Argentino. 3rd Congreso Geológico Chileno, Actas 340-349. Concepción.

Moss, S., Tucker, M.E., 1995. Diagenesis of Barremian–Aptian platform carbonate (The Urgonian Limestone Formation of SE France): near-surface and shallow-burial diagenesis. Sedimentology 42 853-874.

Novara, M., 2003. Caracterización estratigráfica de la Formación Tunal (Paleoceno) en la quebrada El Chorro (departamento La Viña). Comparación con la sección del río Corralito (departamento Rosario de Lerma). Tesis Profesional, Universidad Nacional de Salta (Argentina).

Palma, R.M., 2000. Lacustrine facies in the Upper Cretaceous Balbuena Subgroup (Salta Group): Andina basin, Argentina. In: Gierlowski-Kordesch, E.H., Kelts, K.R. (Eds.), Lake basins through space and time. AAPG Studies in Geology 46, pp. 323-328.

Quattrocchio, M., Ruiz, L., Volkheimer W., 2000. Palynological zonation of the Paleogene of the Colorado and Salta Group basin, Argentina. Revista Española de Micropaleontología 32 61-78.

Reyes, F.C., 1972. Correlaciones en el Cretácico de la cuenca Andina de Bolivia, Perú y Chile. Revista Técnica de Y.P.F. Bolivianos 1(2-3) 101-104.

Riccardi, A.C., 1988. The Cretaceous System of Southern South America. Geological Society of America Memoir 168.

Salfity, J.A., Marquillas, R.A., 1994. Tectonic and sedimentary evolution of the Cretaceous-Eocene Salta Group Basin, Argentina. In: Salfity, J.A. (Ed.), Cretaceous Tectonics of the Andes. Earth Evolution Sciences, Freidr. Vieweg and Sohn, Braunschweig-Weisbaden, pp. 266-315.

Salfity, J.A., Zambrano, J.J., 1990. Cretácico. In: Bonaparte, J.F., Toselli, A.J., Aceñolaza, F.G. (Eds), Geología de América del Sur. Universidad Nacional de Tucumán, Serie Correlación Geológica 2, pp. 185-284.

Sial, A.N., Ferreria, V.P., Toselli, A.J., Parada, M.A., Aceñolaza, F.G., Pimentel, M.M., Alonso, R.N., 2001. Carbon and oxygen isotope compositions of some Upper Cretaceous–Paleocene sequences in Argentina and Chile. International Geological Review 43 892-909.

Tucker, M.E., 1992. The geological record of carbonate rocks. In: Tucker, M.E., Wright, V.P. (Eds.), Carbonate Sedimentology. Blackwell Scientific Publications, London, pp. 401-420.

Veizer, J., 1990. Trace elements and isotopes in sedimentary carbonates. In: Reeder, R.J. (Ed.), Carbonates: Mineralogy and Chemistry. Reviews in Mineralogy 11, pp. 265-299.

Veizer, J., Hoefs, J., 1976. The nature of O18/O16 and C13/C12 secular trends in sedimentary carbonate rocks. Geochimica et Cosmochimica Acta 40 1387-1395.

Warren, J., 2000. Dolomite: occurrence, evolution and economically important associations. Earth-Science Reviews 52 1-82.

Zachos, J.C., Arthur, M.A., Dean, W.E., 1989. Geochemical evidence for suppression of pelagic marine productivity at the Cretaceous/Tertiary boundary. Science 337 61-64.

Zambrano, J.J., 1981. Distribución y evolución de las cuencas sedimentarias en el continente sudamericano durante el Jurásico y el Cretácico. In: Volkheimer, W., Musacchio, E.A. (Eds.), Cuencas Sedimentarias del Jurásico y Cretácico de América del Sur. Comité Sudamericano del Jurásico y Cretácico 1, Buenos Aires, pp. 9-44.

Zambrano, J.J., 1987. Las cuencas sedimentarias de América del Sur durante el Jurásico y Cretácico: su relación con la actividad tectónica y magmática. In: Volkheimer, W. (Ed.), Bioestratigrafía de los sistemas regionales del Jurásico y Cretácico de América del Sur. Comité Sudamericano del Jurásico y Cretácico, Buenos Aires, pp. 1-48.

Figure captions

Fig. 1. Palaeogeographic map of the Yacoraite basin (without palynspastic reconstruction) with location of the sites studied (dots), subbasins (Alemanía, Metán, Lomas de Olmedo, Tres Cruces, and Sey) and structural positive elements (highs and arches) (Salfity and Marquillas, 1994). SJH: Salta-Jujuy High.

Fig. 2. Stratigraphic column and isotopes of the Yacoraite Formation in the Metán subbasin (see Fig. 1 for location). Amblayo, Güemes, Alemanía, and Juramento (J) members are shown.

Fig. 3. Stratigraphic column and isotopes of the Yacoraite Formation in the Huaytiquina section (Sey subbasin, see Fig. 1 for location). As in the stratigraphic column in the Metán subbasin (Fig. 2), the isotope change corresponds to a marked lithological change.

Fig. 4. (a) Landscape of the Cabra Corral area; the solid line indicates the contact between the limestones of the Amblayo Member of the Yacoraite Formation (Y) and underlying sandstones of the Lecho Formation (L). (b) Aspect of the sandstones of the Güemes Member in the Cabra Corral area, composed mainly of thick red sandstone; outcrop thickness 25 m. (c) Outcrop of the Alemanía Member in the Cabra Corral area; arrow indicates a shallowing-upward sequence 4 m thick. (d) Photomicrograph of oolitic grainstone of the Amblayo Member, 1.4 × 0.8 mm. (e) Photomicrograph of oolitic grainstone of the Alemanía Member, 1.4 × 0.8 mm. (f) Photomicrograph of fossiliferous wackestone, 1.1 × 0.7 mm. (g) Green shales and stromatolites of the uppermost Yacoraite Formation. (h) Photomicrograph of a heterolithic limestone, Alemanía Member, 0.9 × 1.2 mm. (i) Photomicrograph of a stromatolite, Alemanía Member, 0.9 × 1.2 mm. (j) Packstone with hummocky cross-stratification, lower Güemes Member. (k) Photomicrograph of packstone, Amblayo Member, 1.4 × 0.8 mm. (l) Photomicrograph of a calcareous sandstone, Amblayo Member, 1.4 × 0.8 mm. (m) Photomicrograph of a silty red sandstone at the base of the Güemes Member, 1.1 × 0.7 mm.

Fig. 5. $\delta^{18}O$ versus $\delta^{13}C$ in carbonates of the Yacoraite Formation in the Metán subbasin. Samples of different members are discriminated (see Fig. 2 for stratigraphic position). Arrows show the main tendency of each member. Samples of the overlying Tunal Formation are also plotted. The Keith and Weber (1964) line discriminating between marine and freshwater limestones is shown.

Fig. 6. Stratigraphic profiles of stable isotope compositions (‰), major elements (%), and ratios of the Yacoraite Formation in the Metán subbasin (see Fig. 2 for location). The carbonate composition (dolomite/calcite, %) is also shown. There is a systematic change toward the contact between the Amblayo and Güemes members. Total Fe was calculated as Fe_2O_3. J, Juramento Member.

Fig. 7. $\delta^{18}O$ versus $\delta^{13}C$ in carbonates of the Yacoraite Formation in the Metán, Sey, and Tres Cruces subbasins (see Fig. 1 for location). Average marine and freshwater limestone fields from Hudson (1977), common range of marine dolomites from Budd (1997), mixing zone dolomites from Choquette and Steinen (1980), and the line to discriminate between marine and freshwater limestones from Keith and Weber (1964).

Fig. 8. Isotope and trace element signatures in carbonates of the Yacoraite Formation in the Metán subbasin (see Fig. 1 for location). The samples are discriminated for each member (see Fig. 2). (A) Sr versus Mn concentrations. (B) $\delta^{13}C$ versus Mn. (C) Na_2O versus SiO_2. (D) K_2O versus SiO_2.

Table 1. Geochemical composition of the Yacoraite limestones in the Metán subbasin (oxides: percentage; elements: ppm). The dolomite/calcite ratio percentage (Dol/Calc) is also shown. *Total Fe was calculated as Fe_2O_3.

Member	Sample	SiO_2	Al_2O_3	CaO	MgO	Na_2O	K_2O	TiO_2	P_2O_5	Fe_2O_3*	LOI	Total	Mn	Sr	Mn/Sr	Mg/Ca	Dol/Calc
Juramento	E37	4.59	0.70	49.16	1.91	0.25	0.09	0.03	0.03	0.64	41.17	98.57	634	1655	0.383	0.039	9
	E36	9.08	2.02	45.03	1.96	0.73	0.35	0.08	0.05	0.55	38.69	98.54	672	1894	0.355	0.044	11
	E35	8.39	1.32	45.91	1.64	0.44	0.24	0.07	0.08	0.58	39.73	98.40	1080	2284	0.473	0.036	7
	E34	6.48	1.48	46.02	2.70	0.48	0.24	0.09	0.05	0.59	40.38	98.51	1255	1254	1.001	0.059	6
	E33	6.58	0.95	44.53	1.25	0.44	0.16	0.07	0.12	0.28	43.55	97.93	526	1215	0.433	0.028	6
Alemanía	E30	7.24	1.14	42.24	6.49	0.07	0.22	0.06	0.01	1.20	40.28	98.95	719	4645	0.155	0.154	50
	C812	25.74	1.14	31.68	6.86	0.00	0.22	0.06	0.00	0.56	32.54	98.80	250	1533	0.163	0.217	29
	E21	6.02	0.88	46.92	3.14	0.09	0.26	0.04	0.01	0.41	40.58	98.35	148	2047	0.072	0.067	48
	C707	2.94	0.42	49.43	2.70	0.08	0.14	0.02	0.04	0.42	42.43	98.62	197	1966	0.100	0.055	10
	C701	13.89	2.70	27.22	12.95	0.40	1.36	0.20	0.03	1.36	38.46	98.57	621	1591	0.390	0.476	86
	C517	7.15	1.59	44.98	3.12	0.39	0.41	0.06	0.13	0.59	39.89	98.31	593	2447	0.242	0.069	12
	A504T	9.89	1.26	37.26	9.18	0.34	0.26	0.05	0.03	1.85	39.50	99.62	1229	2596	0.473	0.246	54
	E16	7.08	1.42	36.63	8.41	2.20	0.25	0.08	0.03	1.80	39.76	97.66	546	4741	0.115	0.290	71
	E15	6.67	0.73	40.86	7.00	0.25	0.14	0.04	0.01	0.96	42.09	98.75	413	5079	0.081	0.171	68
	C402	21.86	2.48	33.11	3.49	0.57	0.80	0.15	0.55	1.40	33.59	98.00	799	2476	0.323	0.112	18
Güemes	C316	10.78	2.12	38.51	4.22	0.91	0.55	0.08	0.03	1.12	38.99	97.31	1625	2204	0.737	0.110	46
	C315	51.73	14.20	7.92	2.35	3.49	2.65	1.05	0.25	4.87	8.99	97.50	1274	651	1.957	0.297	0
	C314	19.65	5.33	36.32	1.14	1.10	0.90	0.29	0.09	1.28	32.56	98.66	1242	4991	0.249	0.045	0
	C313	30.42	8.20	25.98	1.69	2.44	1.61	0.50	0.20	2.05	24.89	97.98	1288	1774	0.726	0.063	0
	C112	9.69	2.44	43.77	0.78	0.83	0.52	0.13	0.14	0.63	40.01	98.94	1441	4175	0.345	0.018	0
	C108	23.60	6.23	32.62	1.22	2.07	1.23	0.31	0.12	1.53	29.10	98.03	1302	1166	1.117	0.037	0
	C102	26.37	5.55	31.31	0.99	1.67	0.96	0.31	0.13	1.14	30.47	98.90	1339	1917	0.698	0.032	4
	K-D	10.04	2.63	45.43	0.68	0.55	0.55	0.12	0.07	0.64	37.38	98.09	1848	1194	1.548	0.015	0
	L06	47.04	9.83	17.70	0.92	3.16	1.81	0.45	0.48	1.72	15.73	98.84	1465	328	4.466	0.052	2
Amblayo	K-G	53.74	13.00	8.60	1.77	4.00	1.92	0.82	0.21	3.55	9.25	96.86	769	527	1.459	0.206	0
	K-I	52.57	11.51	12.97	1.24	2.92	1.51	0.56	0.13	2.57	12.16	98.14	821	999	0.822	0.096	0
	K14-2	30.02	6.45	27.41	1.18	1.87	1.15	0.41	0.15	1.60	27.69	97.93	1985	1189	1.669	0.043	0
	K-J	45.80	7.70	19.97	1.46	2.56	1.18	0.36	0.27	1.98	17.08	98.36	918	884	1.038	0.073	0
	K-K	9.61	2.36	43.06	2.85	0.46	0.51	0.09	0.05	1.49	37.92	98.40	684	1702	0.402	0.066	12
	K-L	21.44	5.30	26.45	8.33	1.46	1.70	0.33	0.06	2.64	31.37	99.08	469	1249	0.376	0.315	71
	K14-1	23.00	4.59	32.77	2.89	1.33	0.82	0.21	0.83	1.47	30.31	98.22	602	1765	0.341	0.088	14
	K-O	34.83	6.80	22.94	4.76	2.52	1.36	0.30	0.09	2.18	22.20	97.98	531	1235	0.430	0.207	29
	E9	5.99	1.31	42.97	5.00	0.37	0.28	0.08	0.03	0.73	42.08	98.84	261	9278	0.028	0.116	26
	E8	8.65	1.73	42.87	3.88	0.49	0.29	0.09	0.03	0.68	39.24	97.95	200	23993	0.008	0.096	12
	E5	11.50	3.15	37.80	5.99	0.78	0.84	0.24	0.05	1.32	37.78	99.45	236	1374	0.172	0.158	53
	E3	7.32	1.51	45.31	2.87	0.47	0.37	0.07	0.03	0.57	41.25	99.77	204	2092	0.098	0.063	6
	E2	16.53	2.98	37.94	3.05	0.84	0.70	0.16	0.04	0.88	35.94	99.06	193	1691	0.114	0.080	55
	E1	8.18	1.74	39.13	7.61	0.39	0.44	0.09	0.03	0.86	41.65	100.12	330	1978	0.167	0.194	36
	Ni-hue	2.33	0.54	50.61	2.31	0.10	0.29	0.02	0.07	0.40	42.74	99.41	237	1431	0.166	0.046	22

Table 2. Isotopic composition of the Yacoraite Formation limestones in the Metán subbasin.

Unit	Sample	$\delta^{18}O_{PDB}$	$\delta^{13}C_{PDB}$
Tunal Fm	CHC17	4.13	-5.57
	CHC01	2.83	-4.63
Juramento	E37	-5.10	-0.15
	E36	-1.91	0.32
	E35	-6.10	-0.81
	E34	-5.79	-0.73
	E33	-3.91	0.39
Alemanía	E30	-0.87	0.95
	C812	0.92	1.20
	E21	0.47	1.51
	C707	0.56	0.83
	C701	3.84	0.50
	C517	0.93	-0.53
	A504T	1.16	-1.91
	E16	3.68	0.02
	E15	1.80	-1.58
	C402	2.01	-2.32
Güemes	C316	0.58	-1.28
	C315	-2.42	-1.50
	C314	-3.02	-2.50
	C313	-2.90	-2.49
	C112	-1.76	-1.49
	C108	-3.05	-1.86
	C102	-1.98	-1.22
	K-D	-2.90	-1.05
	L06	-1.87	-1.30
Amblayo	K-G	-10.02	-3.16
	K-I	-7.07	-2.12
	K14-2	-4.71	-2.03
	K-J	-6.97	-2.16
	K-K	-3.15	-0.41
	K-L	3.69	1.10
	K14-1	-2.16	-0.57
	K-0	-0.42	-0.05
	E9	1.15	1.27
	E8	0.15	1.54
	E5	-0.02	1.34
	E3	0.19	1.57
	E2	0.71	1.48
	E1	1.19	1.88
	Ni-hue	1.29	2.06
	YF8	3.43	2.44
	YF11	2.30	2.43

Table 3. Isotopic composition of the Yacoraite Formation limestones in the Tres Cruces subbasin.

Section	Sample	$\delta^{18}O_{PDB}$	$\delta^{13}C_{PDB}$
Chaupiorco	YF7	-8.74	-5.68
	YF4	-6.68	-4.51
C. Colorada	YF2	-4.34	-2.29
	YF10	3.01	-1.86
Q. Yacoraite	YF56	-8.50	-3.33
	YF60	-0.18	0.84

Table 4. Isotopic composition of the Yacoraite Formation limestones in the Sey subbasin.

Section	Sample	$\delta^{18}O_{PDB}$	$\delta^{13}C_{PDB}$
Coranzulí	YF16	1.67	1.82
	YF18	-6.02	-4.89
Susques	YF23	-4.53	0.03
Huaytiquina	Hu15	-4.61	-5.38
	Hu13a	-4.37	-3.20
	Hu9	-5.85	3.54
	Hu7	-0.14	2.69
	Hu5	-2.99	1.23
	Hu4	-0.39	3.54
	Hu3	-5.20	4.27
Chirincho	YF72	-0.15	-4.39
Q. El Toro	YF5	-6.08	-4.78

Figure 1

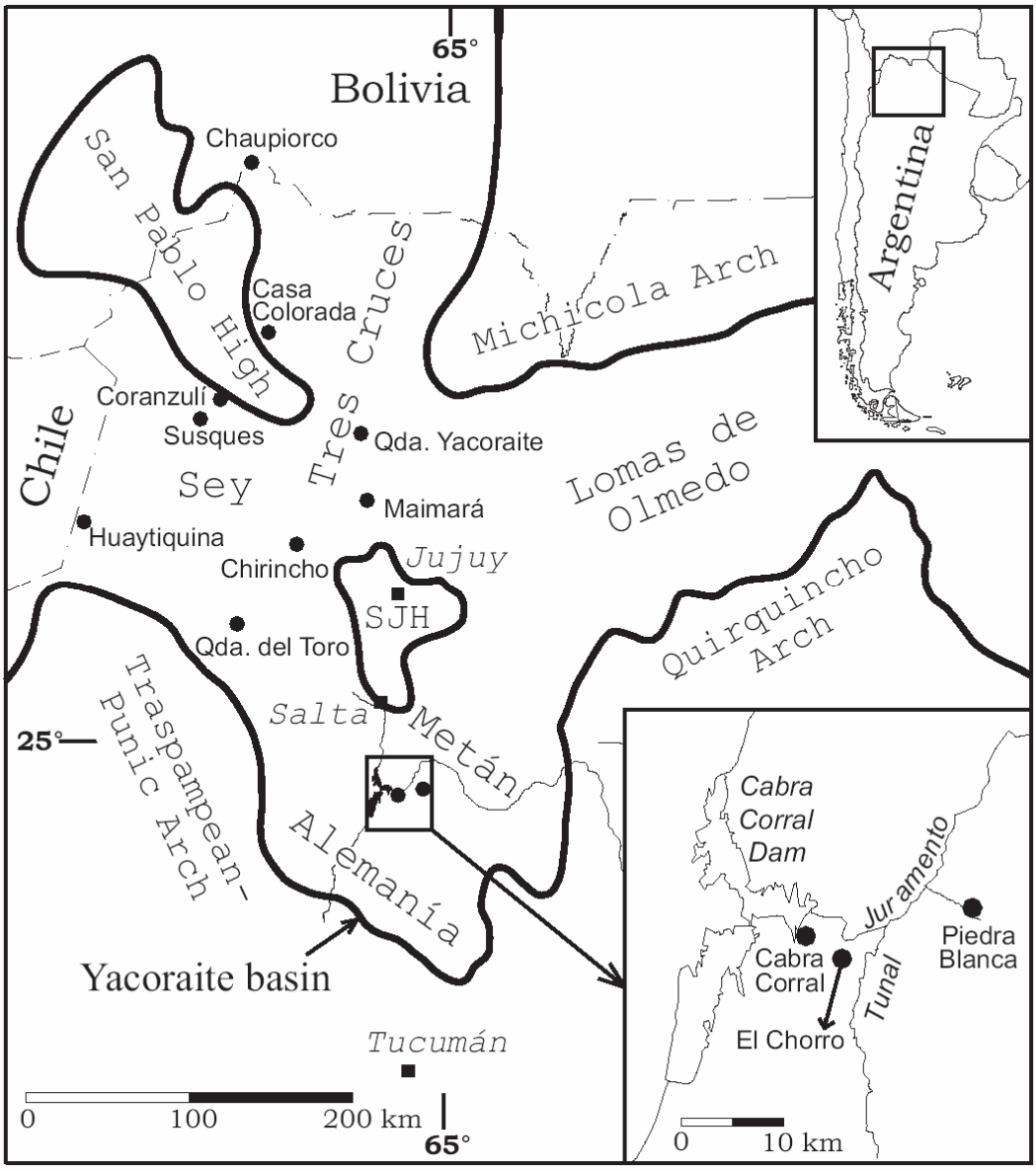

Figure 2

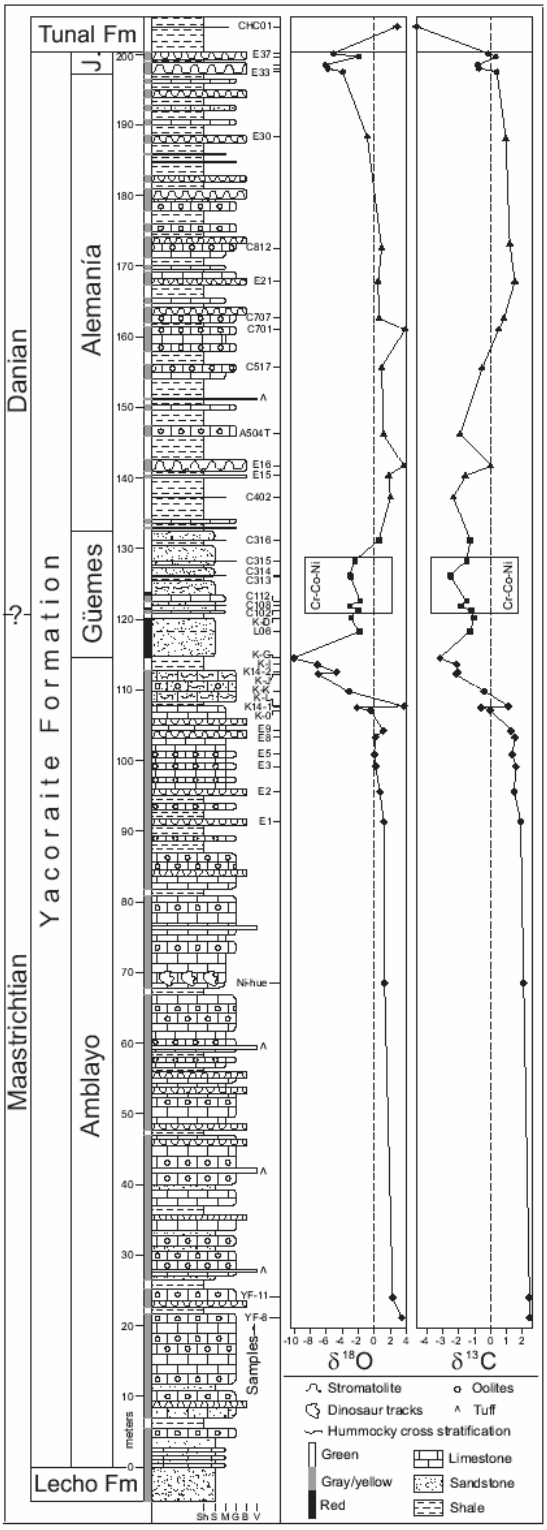

Figure 3

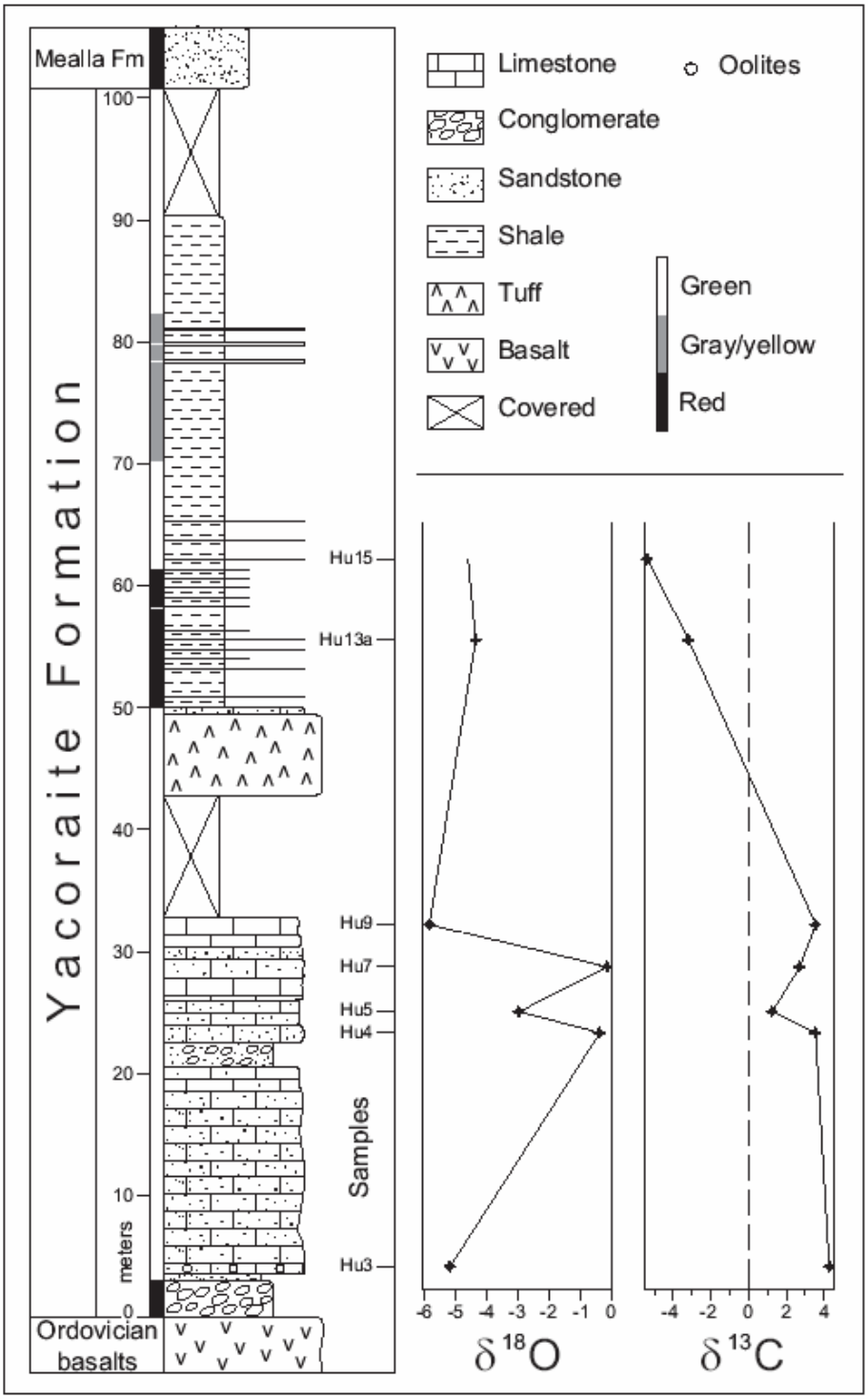
Mealla Fm
Yacoraite Formation
meters
100
90
80
70
60
50
40
30
20
10
0
Hu15
Hu13a
Hu9
Hu7
Hu5
Hu4
Hu3
Samples
Ordovician basalts
Limestone
Oolites
Conglomerate
Sandstone
Shale
Tuff
Basalt
Covered
Green
Gray/yellow
Red
-6 -5 -4 -3 -2 -1 0
δ18O
-4 -2 0 2 4
δ13C

Figure 4a

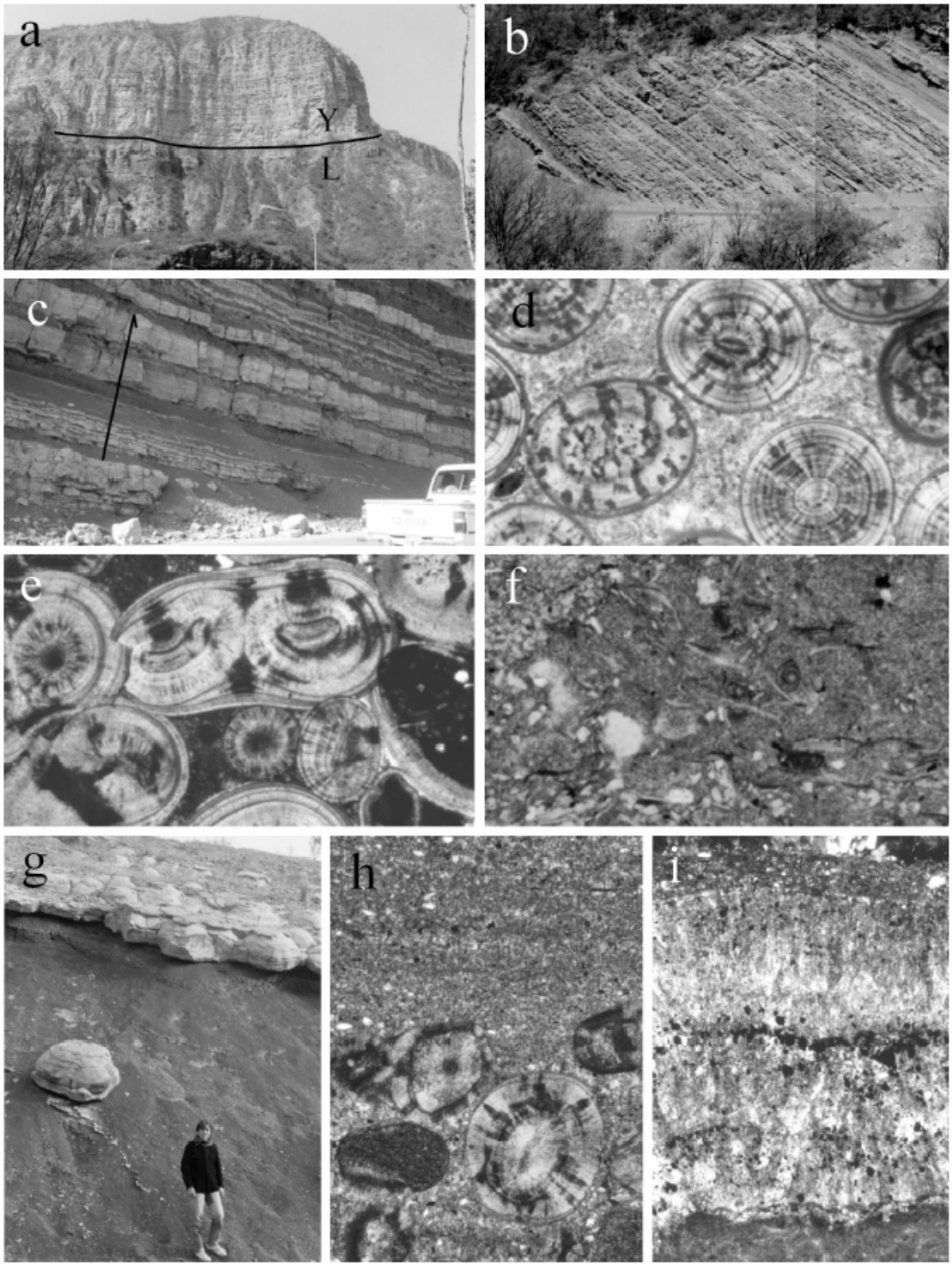

Figure 4b

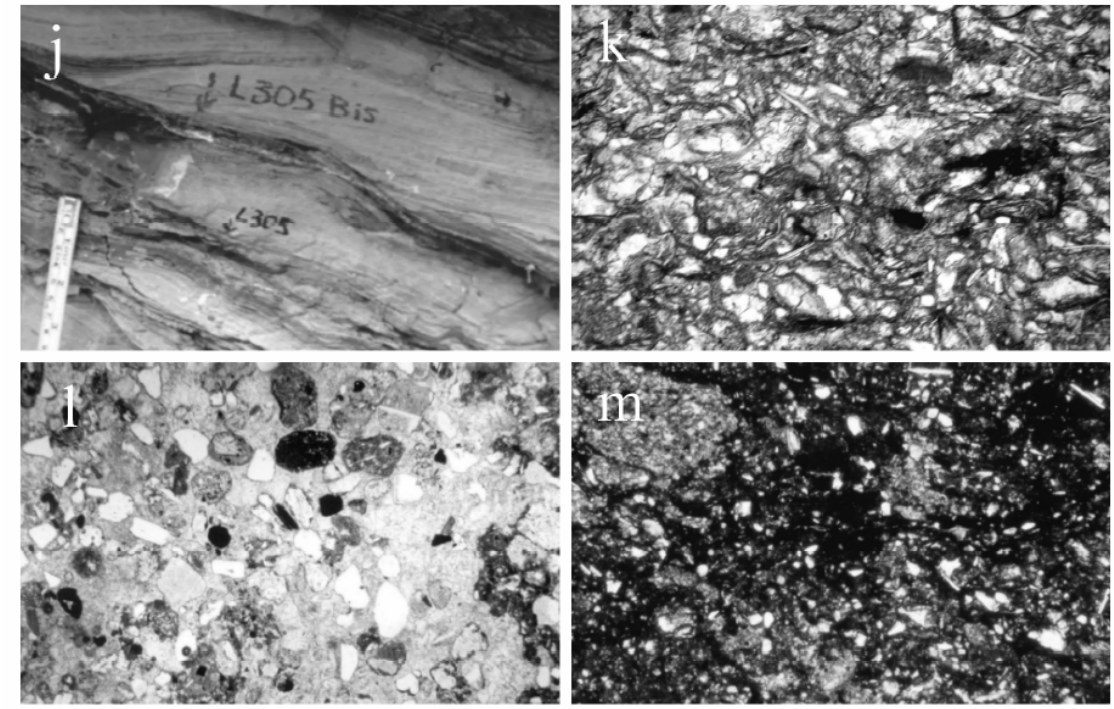

Figure 5

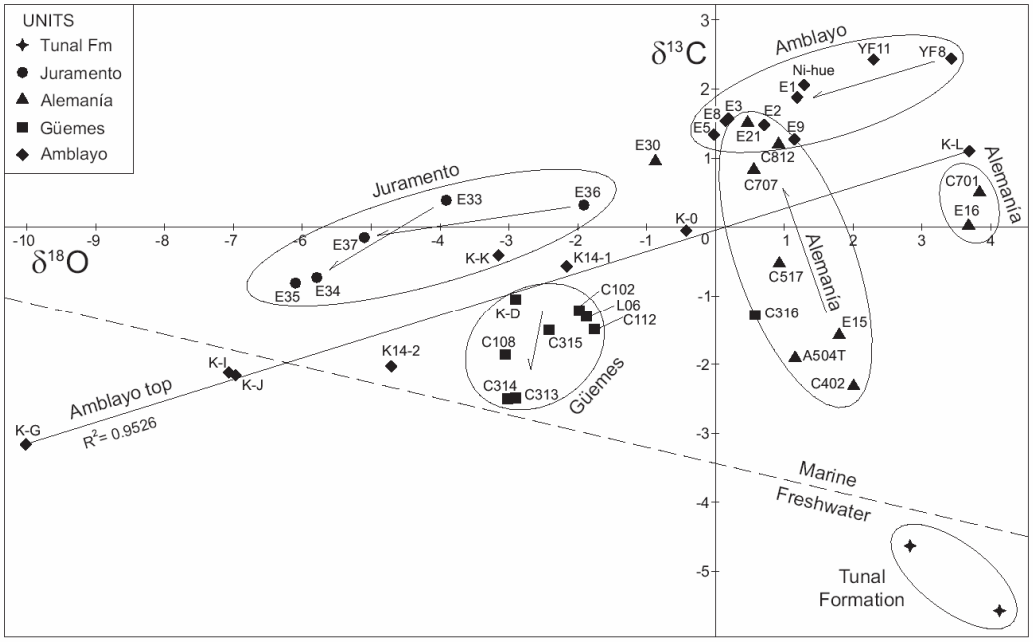

Figure 6a

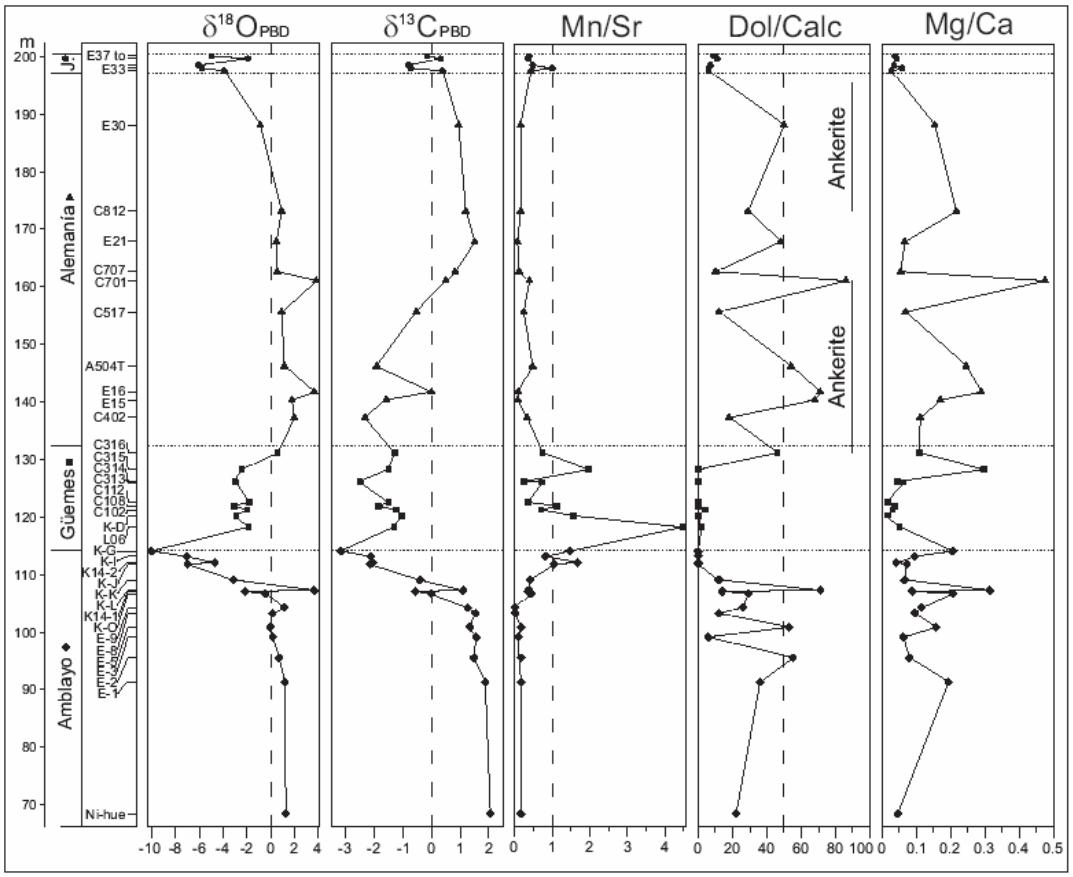

Figure 6b

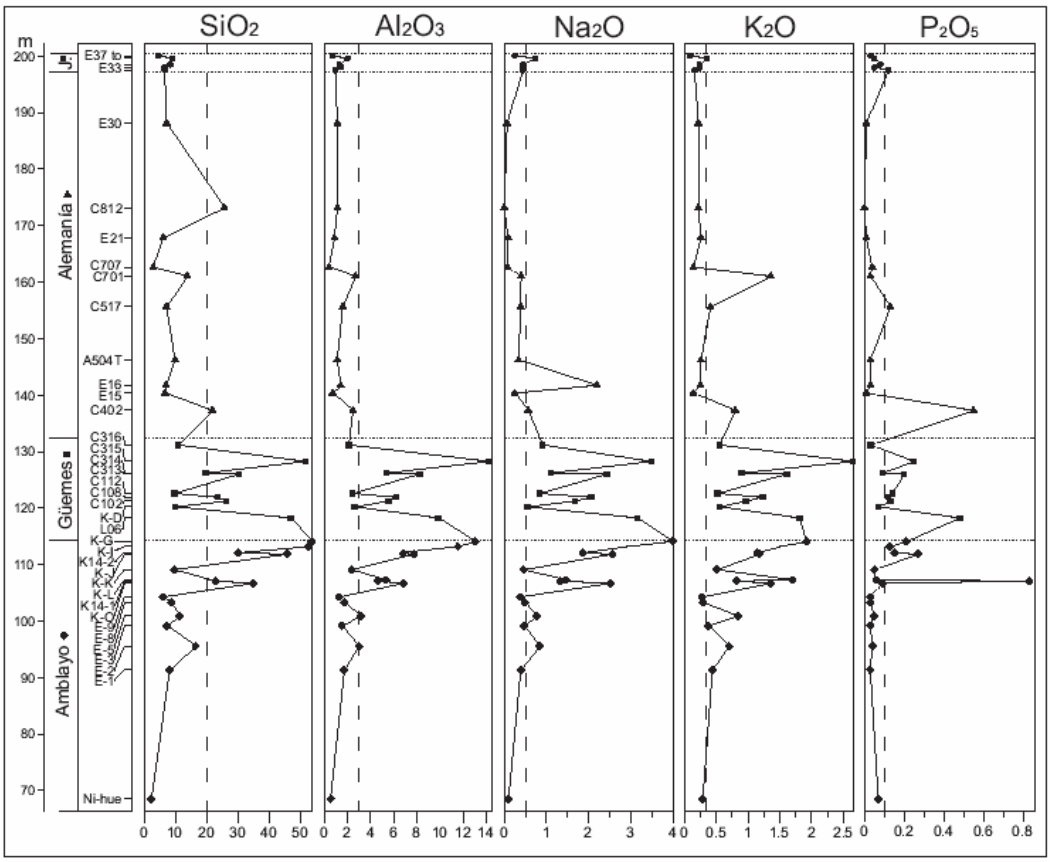

Figure 6c

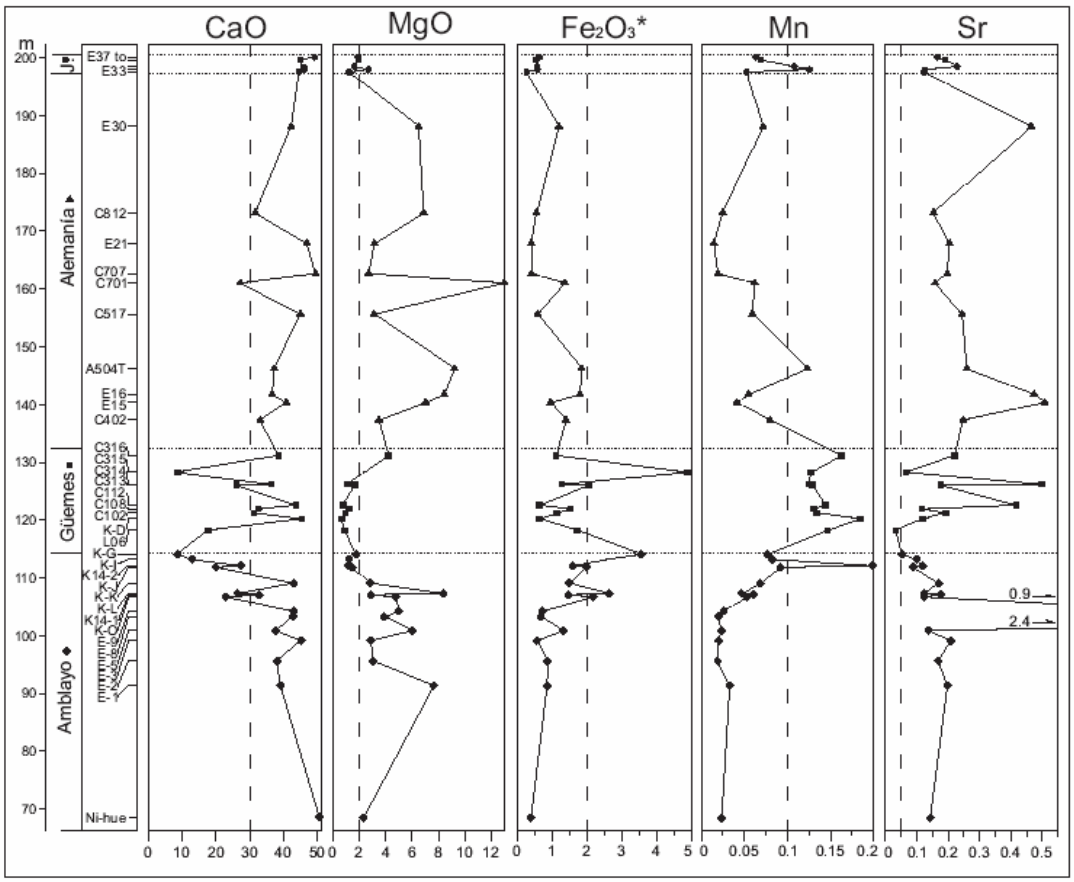

Figure 7

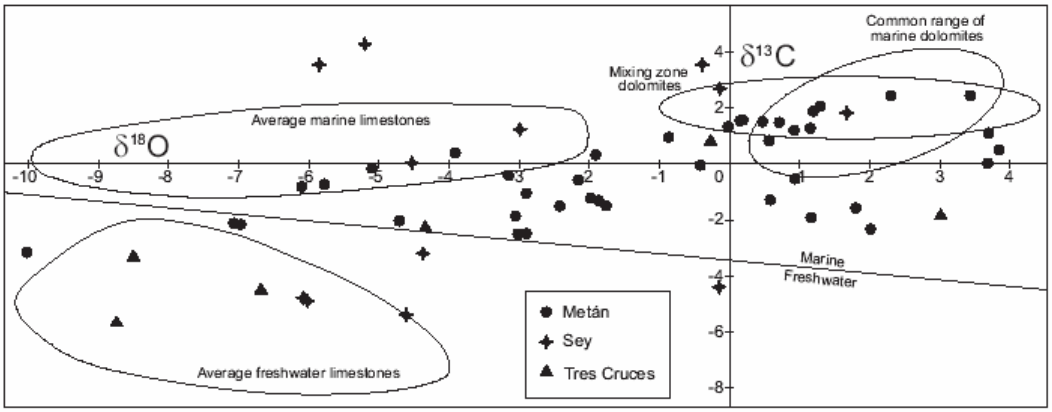

Figure 8